ACS OMEGA

Open Access

http://pubs.acs.org/journal/acsodf

Article

Antitumor Effect of Platinum-Modified STING Agonist MSA-2

Mo Wang, Ya Cai, Tian He, Yuhang Zhang, Lirong Yi, Wenqing Li,* and Peng Zhou*

Cite This: *ACS Omega* 2024, 9, 2650−2656

Read Online

ACCESS | Metrics & More | Article Recommendations | Supporting Information

ABSTRACT: The stimulator of interferon genes (STING)-activated innate immune pathway is strong and durable for tumor immunotherapy. MSA-2 is an available non-nucleotide human STING agonist that promotes the tumor immunotherapy of STING activation. However, strategies for remolding and improving the immunotherapy effects of MSA-2 are of value for clinical applications. Here, we synthesized the platinum salt-modified MSA-2 (MSA-2-Pt) due to platinum salt being a classic chemotherapeutic drug. We found that MSA-2-Pt could achieve double-effect antitumor immunotherapy, including inducing cell death by platinum and activating the STING pathway by MSA-2. In the colon carcinoma MC38 model (sensitive to immune checkpoint immunotherapy tumor) and melanoma B16F10 model (poorly immunogenic and highly aggressive tumor), the MSA-2-Pt had a good antitumor effect, which was a little better than MSA-2 with intratumor injections. The results present a promising strategy for STING activation in tumor immunotherapy and broadening platinum-based drugs.

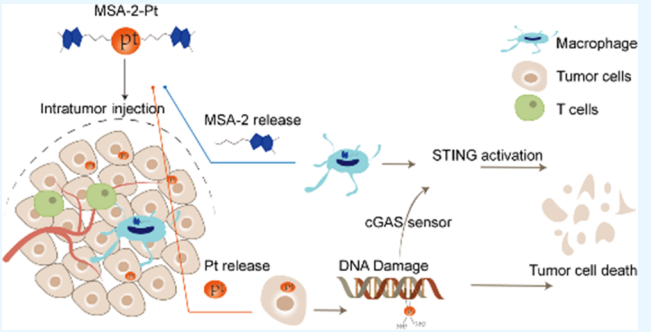

1. INTRODUCTION

Immunotherapy is becoming a powerful clinical strategy for cancer treatment, including immune checkpoint inhibitors,[1,2] cytokines,[3,4] engineered T cell therapies,[5−7] oncolytic viruses,[8,9] bispecific antibodies,[10] and nano-immunotherapy.[11,12] In the numerous immunotherapy strategies, the cGAS-STING signaling pathway plays a remarkable role in the antitumor immune response and antipathogen host defense.[13] The cyclic guanosine monophosphate-adenosine monophosphate synthase (cGAS) is a cytosolic DNA sensor[14] that synthesizes cyclic dinucleotides (CDNs, 2′,3′-cyclic GMP-AMP (2′,3′-cGAMP)) binding downstream STING proteins, which are transferred from the ER to the Golgi apparatus and activate TANK-binding kinase 1 (TBK1) and IkB kinase (IKK).[15,16] These kinases activate the transcription factor interferon regulator (IRF 3) and NF-kB, respectively, to induce the production of type I interferon and other cytokines[17] and initiate an antitumor effect.[18−20]

Initial STING agonist small molecules were derivatives of the CDN,[21,22] however, with poor stability and cell impermeability of properties.[22] An oral non-CDN STING agonist, MSA-2 is a small molecule that activates STING and achieves antitumor immunotherapy, which has a wide prospect for STING-mediated immunotherapy.[23,24] Recently, sono-driven STING activation using self-assembled nanoparticles from a sonodynamic semiconducting polymer core conjugated with MSA-2 performed a precision sono-immunotherapy.[25] Selenium-inserting STING agonists (MSA-2) displayed available antitumor agent.[26] Therefore, strategies for remolding and improving the immunotherapy effects of MSA-2 are of value for clinical applications.

Platinum (Pt)-based drugs are the most classic chemotherapy drug widely used for the treatment of various solid tumors such as genitourinary, colorectal, and nonsmall cell lung cancers.[27] Cisplatin is the leading anticancer drug, which is developed into classical Pt(II) drugs (carboplatin, oxaliplatin, lobaplatin, nedaplatin, etc.), and nonclassical Pt(II) drugs (picoplatin, BBR3464, 56MESS) and Pt(IV) prodrugs (satraplatin and Pt(IV)-azide complexes).[28] Various modalities and recent advances in combination with platinum-based antitumor therapy were developed, for instances, platinum drugs combined with surgery, chemotherapy, radiation therapy, thermal therapy, gene editing, ROS-based therapy, and immunotherapy.[28,29] The platinum-based drug not only caused tumor cell death and remodeled the immunosuppressive microenvironment[30] but also activated the cGAS-STING pathway in immune cells to enhance the antitumor immune response.[31,32] Therefore, we first synthesized a platinum-modified STING agonist MSA-2 (MSA-2-Pt) and supposed that it could induce cell death by Pt and activate the STING pathway by MSA-2.

In this study, we found that MSA-2-Pt could induce cell death by Pt and activate the STING pathway by MSA-2, which showed a good antitumor effect. The results present a promising strategy for STING activation of tumor immunotherapy.

Received: September 28, 2023
Revised: December 18, 2023
Accepted: December 21, 2023
Published: January 3, 2024

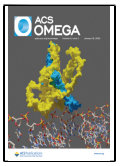

2. MATERIALS AND METHODS

2.1. Cell Culture. Mouse macrophage cell line RAW264.7 and melanoma B16F10 cell line was purchased from the Cell Bank of the Chinese Academy of Sciences (Shanghai, China). Mouse colon adenocarcinoma cell line MC38 was purchased from the Cell Resource Center, Peking Union Medical College (National Science & Technology Infrastructure-National BioMedical Cell-Line Resource, NSTI-BMCR, Beijing, China). The cells were cultured in DMEM (Gibco) with 10% FBS and 1% penicillin−streptomycin at 37 °C in an incubator with 5% CO_2.

2.2. Animals. Male C57BL/6 mice (6−8 weeks) were purchased from Charles River Company and fed in the Laboratory Animal Center of Nantong University. The mouse experimental procedures were approved by the Institutional Animal Care and Use Committee of the Nantong Medical School, Nantong University, China.

2.3. Cell Viability. The MC38 cells were seeded into 96-well plates with 10000 cells/well. After 24 h, the MC38 cells were treated with control (DMSO) or 25, 50, 75, 100, 200, or 300 μM MSA-2 or MSA-2-Pt. After 24 h, 10 μL of CCK8 test solution (CELL COUNTING KIT-8, CK04, DOJINDO, China) was added to each well and incubated at 37 °C for 1 h, and the absorbance was measured at 450 nm by a microplate reader (Synergy HITX Multi-Mode Reader, BioTek).

2.4. Cell Images. The MC38 cells were seeded into a 24-well plate with 1×10^5 cells/well. After 24 h, the MC38 cells were treated with control (DMSO) or 75 μM MSA-2 or MSA-2-Pt for 12 and 24 h. The cell images were captured under an inverted microscope.

2.5. ELISA Assay for IFN-β. RAW264.7 cells were seeded into a 24-well plate with 1×10^5 cells/well. After 24 h, the RAW264.7 cells were treated with control (DMSO), 10, 50 μM MSA-2 or MSA-2-Pt for 24 h. The levels of INF-β in the medium were tested by a mouse IFN-β ELISA Kit (Cat: MM-0124M1, Meimian, China).

2.6. Western Blot Analysis. The RAW264.7 cells were seeded into a 6 cm plate with 5×10^5 cells/plate. After 24 h, the RAW264.7 cells were treated with control (DMSO) or 10, 25, and 50 μM MSA-2 or MSA-2-Pt for 3 h. RAW264.7 cells were collected and lysed by in RIPA Lysis Buffer (Beyotime) containing phenylmethanesulfonyl fluoride (PMSF) and protease inhibitor cocktail (Roche) on ice for 30 min. Protein lysates were resolved by SDS-PAGE and electrotransferred to a nitrocellulose membrane. β-Actin (Cat: 66009-1-Ig, Proteintech, 1:5000) was the inner control. The primary antibodies were Phospho-STING (Ser365) (D8F4W) (Cat: 72971, Cell Signaling Technology, 1:1000), Phospho-TBK1/NAK (Ser172) (D52C2) (Cat: 5483, Cell Signaling Technology, 1:1000), Phospho-NF-κB p65 (Ser536) (93H1) (Cat: 3033, Cell Signaling Technology, 1:1000), Phospho-IRF-3 (Ser396) (D6O1M) (Cat: 29047, Cell Signaling Technology, 1:1000), Rabbit mAb 29047, TMEM173/STING Polyclonal antibody (Cat: 19851-1-AP, Proteintech, 1:1000). The secondary antibodies (Cat: ab216777, abcam, 1:5000; Cat: ab216776, abcam, 1:5000) were used. An imaging system (Amersham Typhoon) was used to detect the signal.

2.7. MSA-2-Pt Treatment. MC38 cells (2×10^5 per mouse) were injected subcutaneously into 6-week-old female C57BL/6 mice to establish tumor models. When the tumor volumes reached about 100 mm^3, the mice were randomly divided into 3 groups: control, MSA-2, MSA-2-Pt (n = 5 each group). The mice were intratumor (i.t.) injected with a single dose of control, 150 μg MSA-2, and 150 μg MSA-2-Pt. After 1 day, the mice were sacrificed. The blood were collected to obtain plasma serum by centrifuging (3000 rpm, 15 min) for blood biochemical examination. Tumors were harvested and fixed with a MDF stationary liquid for pathological analysis.

2.8. Histological Analysis. The tumor of mice were fixed by MDF stationary liquid, then paraffin embedding, slicing, and staining with Hematoxylin−Eosin (H&E) staining kit (E607318, Sangon Biotech, China). The images were obtained under an optical microscope (Leica DM2000, Germany).

2.9. Immunofluorescence Staining. The tumor tissue of mice was fixed by MDF stationary liquid, paraffin embedding, and slicing. Briefly, paraffin was removed and rehydrated tissue. Antigen retrieval was performed. Permeabilization was carried out with 0.1% Triton X-100. The reagent was blocked with 5% BSA for 1 h at room temperature. Staining with the primary antibody: CD4 antibody (Cat: ab183685, Abcam), CD8 α antibody (Cat: ab217344 Abcam). Secondary antibody: goat anti-Rabbit IgG (H + L) cross-adsorbed secondary antibody, Alexa Fluor 488 (A11008, Life Technologies Corporation, 1:200) at room temperature for 2 h. Nuclei were counterstained using DAPI (Abcam, ab104139). The images were obtained with a fluorescence microscope (ZEISS, Oberkochen, Germany).

2.10. Antitumor Effect of MSA-2-Pt. MC38 cells (2×10^5 per mouse) were injected subcutaneously into 6-week old female C57BL/6 mice to establish tumor models. When the tumor volumes reached about 100 mm^3, the mice were randomly divided into 3 groups: control, MSA-2, and MSA-2-Pt (n = 9 each group). The mice were intratumor (i.t.) injected with control, 150 μg of MSA-2, and 150 μg of MSA-2-Pt for three doses as Figure 5A.

B16F10 cells (2×10^5 per mouse) were injected subcutaneously into 6-week old female C57BL/6 mice to establish tumor models. When the tumor volumes reached about 100 mm^3, the mice were randomly divided into 3 groups: control, MSA-2, and MSA-2-Pt (n = 9 each group). The mice were intratumor (i.t.) injected with control, 150 μg of MSA-2, 150 μg of MSA-2-Pt for three doses as Figure 6A. Tumor size was measured with a digital caliper every 3 days and calculated the volume (length × width × width/2). Mice were sacrificed when the tumor size reached 1.6 cm in diameter.

B16F10 cells (5×10^5 per mouse) were injected subcutaneously into 6-week old female C57BL/6 mice to establish tumor models. When the tumor volumes reached about 100 mm^3, the mice were randomly divided into 4 groups: control, MSA-2, MSA-2-Pt, and cisplatin (n = 10 each group). The mice were intratumor (i.t.) injected with control, 150 μg of MSA-2, 150 μg of MSA-2-Pt, and cisplatin (Sigma, P4394) for three doses.

2.11. Effects of CD8+ T Cell Depletion on Immunotherapy of MSA-2-Pt Treatment. Female C57BL/6 mice were subcutaneously inoculated with B16F10 cells (2×10^5/mouse). After the tumor size reached about 100 mm^3, the mice were divided into 2 treatment groups, including αCD8 + MSA-2-Pt and IgG + MSA-2-Pt. The αCD8 + MSA-2-Pt group was treated with antimouse CD8α (α-CD8, Bioxcell, BE0004-1, 200 μg per mouse, i.p.) + MSA-2-Pt (i.t. 150 μg/mouse, n = 10). IgG + MSA-2-Pt group were i.t. injected with isotype control antibody (Bioxcell, Catalog # BP0090, 200 μg per mouse,i.p.) + MSA-2-Pt (i.t. 150 μg/mouse, n = 10) for three doses.

https://doi.org/10.1021/acsomega.3c07498
ACS Omega 2024, 9, 2650−2656

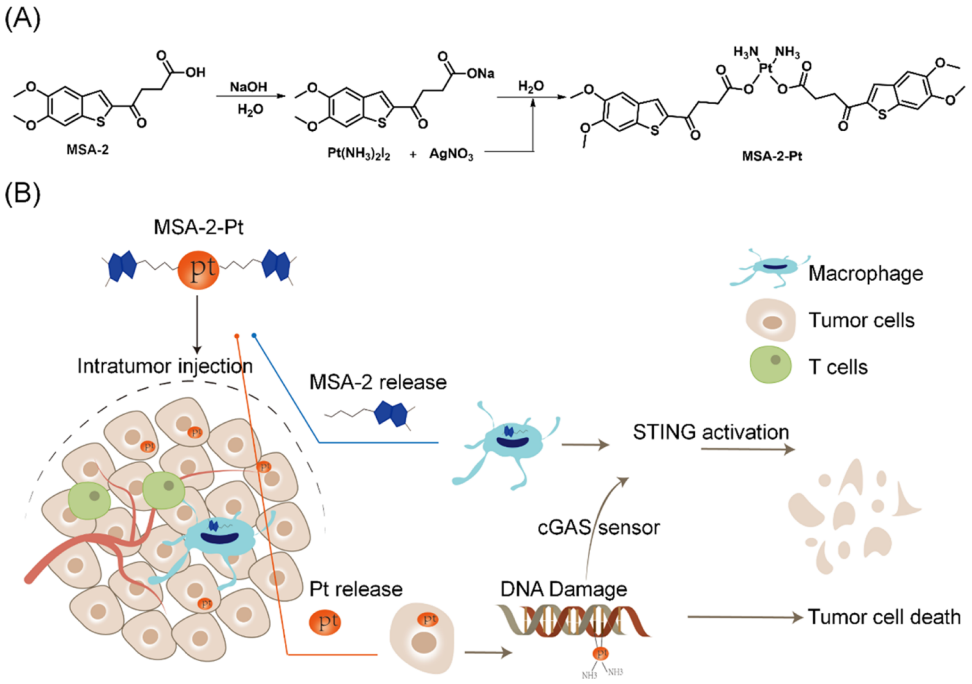

Figure 1. (A) Illustration of the synthesis steps of MSA-2-Pt. (B) MSA-2-Pt could release MSA-2 and Pt in the tumor. (1) Pt could induce cell death, which might release damaged DNA to activate the cGAS-STING pathway. (2) MSA-2-Pt could activate the STING pathway directly by MSA-2.

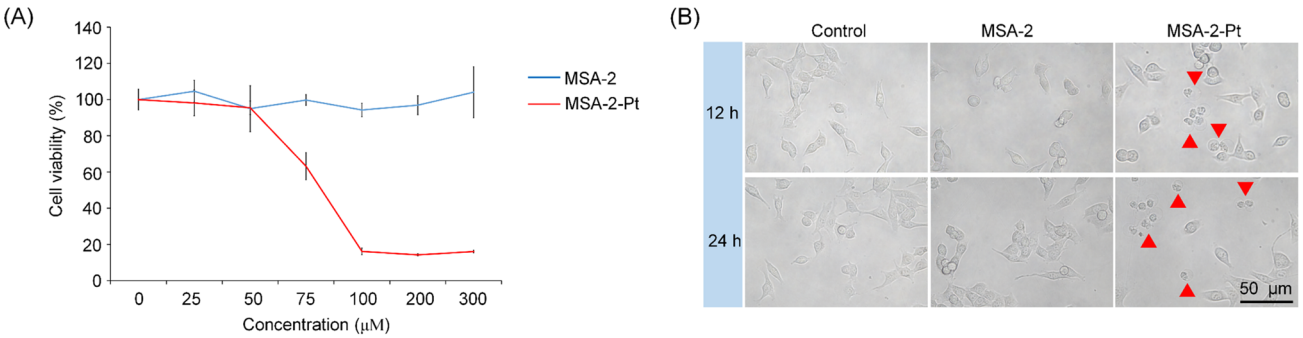

Figure 2. (A) Cell viability of MC38 cells of MSA-2 and MSA-2-Pt treatment. Data presented are mean ± SD. (B) Microscopic images of the MC38 cells treated with 75 μM MSA-2 and MSA-2-Pt for 12 and 24 h (n = 3).

2.12. Statistical Analysis. Data were expressed as mean ± SEM. All statistical analyses were performed using GraphPad Prism 8.0 software (GraphPad Software). A one-way ANOVA analysis was used to determine the statistical significance (no significance, n.s. $P < 0.05$, *$P < 0.05$, **$P < 0.01$, ***$P < 0.001$).

3. RESULTS AND DISCUSSION

3.1. Synthesis of MSA-2-Pt. Platinum (Pt)-based drugs are the most widely used chemotherapy drugs for various solid tumors.[33] Here, MSA-2-Pt was synthesized as outlined in Figure 1A, and the ^{1}H NMR and ^{13}C NMR spectrum data showed the characterizations of MSA-2-Pt (Figures S1 and S2). The MSA-2-Pt could decompose a Pt and two MSA-2 *in vitro* and *in vivo*. Here, we supposed that MSA-2-Pt could achieve double-effect antitumor immunotherapy. MSA-2-Pt could induce cell death by Pt, which might release damaged DNA to activate the cGAS-STING pathway. MSA-2-Pt could activate the STING pathway directly by MSA-2 (Figure 1B).

3.2. MSA-2-Pt Induced Cell Death *In Vitro*. Due to MSA-2-Pt including Pt, it might cause cell death by Pt. The cell viability of MC38 cells treated with MSA-2 and MSA-2-Pt was tested by the CCK8 assay. The results showed that MSA-2-Pt induced cell death significantly from 75 μM, which showed a dose-dependent response (Figure 2A). However, MSA-2 did not cause cell death until 300 μM (Figure 2A). Then, the microscope images also showed that the MSA-2-Pt induced cell death significantly with 75 μM from 12 to 24 h, which exhibited typical cell pyroptosis (Figure 2B). The MSA-2 did not cause cell death (Figure 2B). Also, we have investigated the cell viability of MC38 cells and B16F10 treated with MSA-2, cisplatin, and MSA-2-Pt. The results showed MSA-2-Pt induced cell death significantly from 75 μM with a dose-dependent manner. The toxicity of MSA-2-Pt was a little more than that of cisplatin (Figures S3 and S4). These results indicated that MSA-2-Pt could induce tumor cell death.

3.3. MSA-2-Pt Mediated STING Pathway Activation *In Vitro*. The activation of the cGAS-STING pathway triggers a series of downstream signaling events, including stimulation and recruitment of TANK-binding kinase 1 (TBK1) and interferon regulatory factor 3 (IRF 3). The activation of STING can result in the type I interferon signaling cascade and production of other immune factors.[22] To explore the activation of the STING

https://doi.org/10.1021/acsomega.3c07498
ACS Omega 2024, 9, 2650−2656

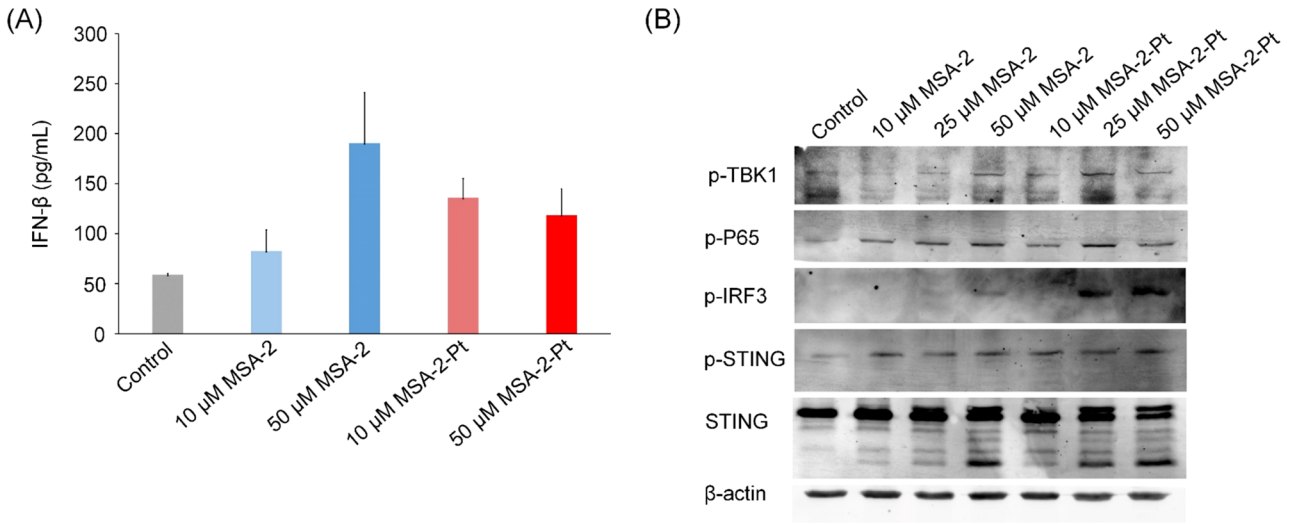

Figure 3. (A) Levels of IFN-β in culture media of RAW264.7 cells with different concentrations of MSA-2 and MSA-2-Pt treatment for 24 h were determined by using the ELISA kit. Data presented are mean ± SEM. (B) Western blot analysis of related proteins in RAW264.7 cells treated with control (DMSO), MSA-2, and MSA-2-Pt after 3 h (n = 3).

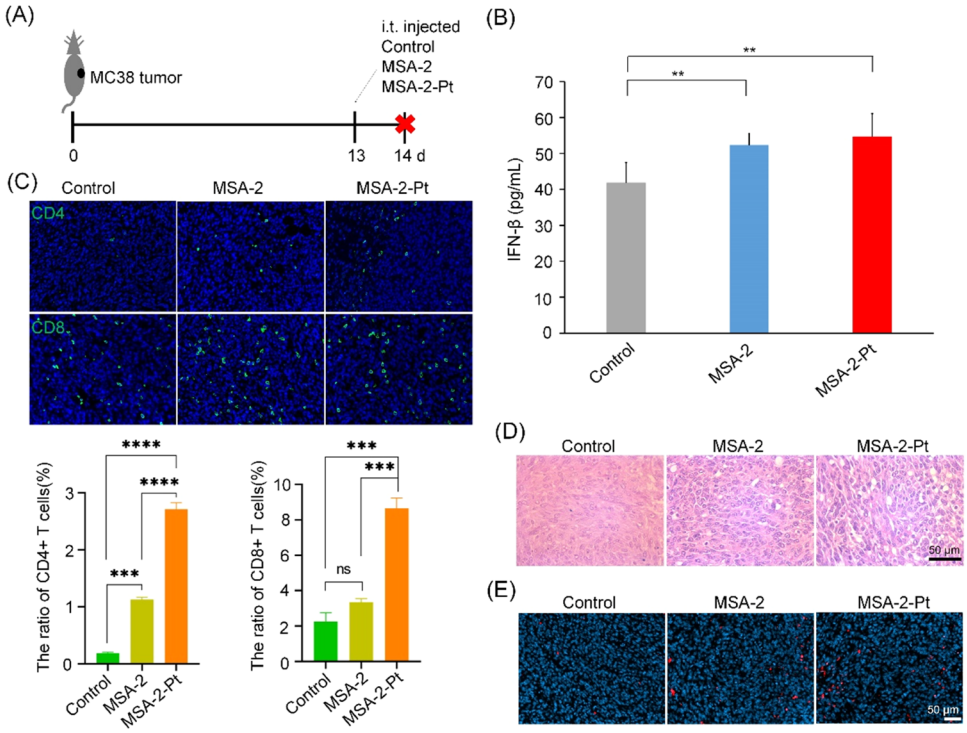

Figure 4. (A) Treatment plan for antitumor effect after a single i.t. injection with control, MSA-2, or MSA-2-Pt. (B) The level of IFN-β in mouse serum were measured by ELISA after a single i.t. injection with control, MSA-2, or MSA-2-Pt. (n = 5). **P < 0.01. (C) Immunohistological staining of CD4+ and CD8+ T cells in tumors after a single i.t. injection with control, MSA-2, or MSA-2-Pt (n = 5). The number of CD4+ T, CD8+ T cells, and tumor cells were counted by using ImageJ software from immunofluorescence images of tumor tissue sections (n = 5). The ratio of CD4+ T cells and CD8+ T cells/total cells was calculated in panel (C) in the revised manuscript. Statistical analysis was performed using the one-way ANOVA. (D) HE staining of the tumors after a single i.t. injection with control, MSA-2, or MSA-2-Pt (n = 5). (E) TUNEL assay of the tumors after a single i.t. injection with control, MSA-2, or MSA-2-Pt (n = 5).

pathway, we treated the mouse macrophage cell line RAW264.7 with different concentrations of MSA-2 and MSA-2-Pt. We found that both of them could trigger the secretion of IFN-β (Figure 3A). We also investigated the activation of the STING pathway. The results showed that phosphorylated P65 (P-P65) were increased in MSA-2-Pt- and MSA-2-treated RAW264.7 cells compared to control (Figure 3B). The above results indicated that MSA-Pt could activate the STING pathway the same way as MSA-2, which showed its function in tumor immunotherapy.

3.4. MSA-2-Pt Induced Cell Death and Activated the STING Pathway *In Vivo*. The MSA-2-Pt could induce cell death and activate the STING pathway *in vitro* in the above results. Therefore, we investigated the effect of MSA-2-Pt in a subcutaneous MC38 tumor model *in vivo* (Figure 4A). We found that MSA-2-Pt was similar to MSA-2 promoting the levels

https://doi.org/10.1021/acsomega.3c07498
ACS Omega 2024, 9, 2650−2656

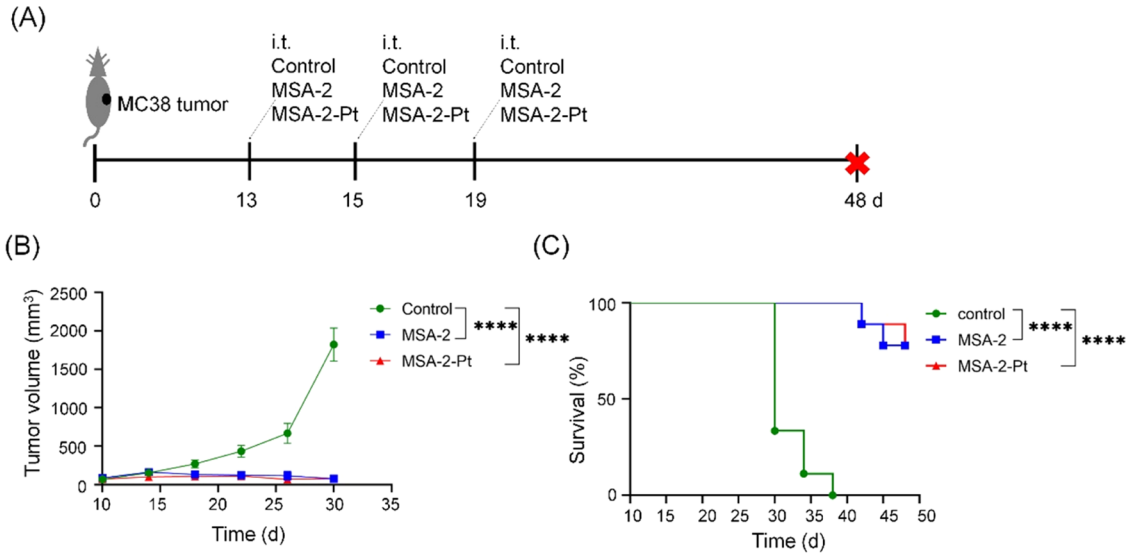

Figure 5. (A) Schematic illustration of the MC38 tumor models and the treatment strategy. (B, C) Tumor volumes (B), and survival percent (C) after intratumor injected (i.t.) with control, 150 μg of MSA-2, 150 μg of MSA-2-Pt for three doses as (A) (n = 9 for each group). Data presented the mean ± SEM. Statistical significance in panel (B) was analyzed with one-way ANOVA. Statistical significance in panel (C) was analyzed using the log-rank (Mantel-Cox) test. ****P < 0.0001.

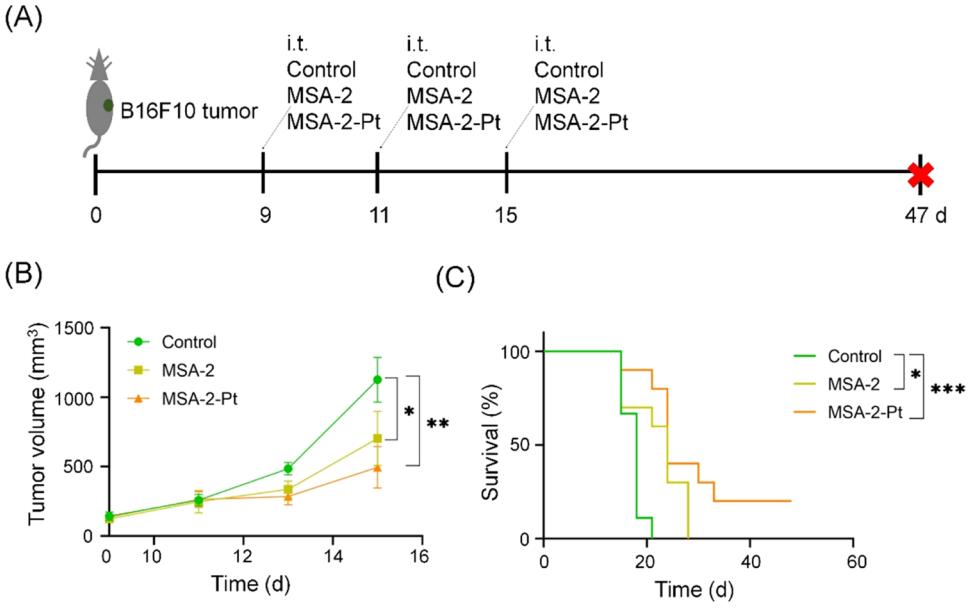

Figure 6. (A) Schematic illustration of the B16F10 tumor models and the treatment strategy. (B, C) Tumor volumes (B), and survival percent (C) after intratumor injected (i.t.) with control, 150 μg of MSA-2, and 150 μg of MSA-2-Pt for three doses as (A) (n = 10 for each group). Data presented as the mean ± SEM. Statistical significance in panel (B) was analyzed with one-way ANOVA. Statistical significance in panel (C) was analyzed using the log-rank (Mantel-Cox) test. *P < 0.05; **P < 0.01; ***P < 0.001.

of IFN-β in mouse serum after a single i.t. injection with MSA-2-Pt or MSA-2, compared with the control group (Figure 4B). Activation of STING with agonists enhances the infiltration and activity of cytotoxic T cells in tumors, contributing to the induction of tumor regression. To further confirm the immunity activation of MSA-2-Pt, immunohistological staining proved that MSA-2-Pt effectively increased the proportion of CD4-positive cells and CD8-positive cells to the same extent with MSA-2 compared with that of the control group (Figure 4C). MSA-2-Pt could divide Pt and MSA-2-Pt induced tumor cell death, which might release damaged DNA to activate the cGAS-STING pathway. MSA-2 could activate the STING pathway directly. MSA-2-Pt effectively increased the proportion of CD4-positive cells and CD8-positive cells. The CD8+ T cells killed tumor cells. Hematoxylin−eosin (H&E) staining of tumor sections showed that tumor cells were dead significantly with MSA-2-Pt and MSA-2 treatment compared to the control (Figure 4D). TUNEL staining of tumor sections showed a significantly higher proportion of tumor cell apoptosis with MSA-Pt and MSA-2 treatment (Figure 4E). The results indicated that MSA-2-Pt could activate STING-mediated immunotherapy and cause cell death.

3.5. Antitumor Effect of MSA-2-Pt. Finally, we administrated the antitumor effect of MSA-2-Pt on the MC38 (colon carcinoma) tumor model, which was sensitive to the immune checkpoint immunotherapy model. The MC38 tumor model

https://doi.org/10.1021/acsomega.3c07498
ACS Omega 2024, 9, 2650−2656

was treated with MSA-2-Pt as the treatment strategy (Figure 5A). Tumor growth was measured for 48 days (Figure 5B). Treatment with MSA-2-Pt and MSA-2 significantly reduced tumor growth (Figure 5B) and increased survival (Figure 5C) when compared to the control group. Importantly, there were 7 out of 9 mice tumor-free with MSA-2-Pt treatment.

Next, we investigated a poorly immunogenic and highly aggressive melanoma tumor B16F10 model. The B16F10 tumor model was treated with MSA-2-Pt as the treatment strategy (Figure 6A). Tumor growth was measured, and animal survivals measured. Treatment with MSA-2-Pt and MSA-2 significantly reduced tumor growth (Figure 6B) and increased survival (Figure 6C) when compared with the control group. Importantly, there were 2 mice tumor-free with MSA-2-Pt treatment. We added cisplatin treatment in the B16F10 tumor model to elevate the antitumor effect of the MSA-2, cisplatin, and MSA-2-Pt treatment. The tumor growth was shown in Figure S5. The tumor growth was significantly decreased with MSA-2-Pt treated compared with MSA-2 and cisplatin. We also used the CD8+ depletion antibody to investigate the effects of CD8+ T cell depletion on immunotherapy of MSA-2-Pt treatment. The tumor growth was increased significantly in anti-CD8α + MSA-2-Pt compared to that in IgG + MSA-2-Pt (Figure S6), which indicated that the MSA-2-Pt activated the CD8 T cells to antitumor.

4. CONCLUSIONS

In summary, MSA-2 is an oral non-CDN STING agonist, which is a small molecule and has good cell membrane permeability that activates STING and achieves antitumor immunotherapy. It has attracted much attention for its STING-mediated immunotherapy. Here, The MSA-2-Pt was a platinum-modified MSA-2. MSA-2-Pt could induce cell death by Pt, which might release damaged DNA to activate the cGAS-STING pathway. Besides, MSA-2-Pt could activate the STING pathway directly by MSA-2. It will broaden platinum-based drugs for tumor therapy.

■ ASSOCIATED CONTENT

Supporting Information

The Supporting Information is available free of charge at https://pubs.acs.org/doi/10.1021/acsomega.3c07498.

Preparation of platinum(II) coordination compounds MSA-2-Pt; ^{1}H NMR spectra of MSA-2-Pt; ^{1}H NMR spectra of MSA-2-Pt; cell viability of MC38 with MSA-2, cisplatin, and MSA-2-Pt treatment; cell viability of B16F10 with MSA-2, cisplatin, and MSA-2-Pt treatment; B16F10 tumor growth was treated with the MSA-2, cisplatin, and MSA-2-Pt treatment; and effect of CD8+ T cell depletion on immunotherapy of MSA-2-Pt treatment (PDF)

■ AUTHOR INFORMATION

Corresponding Authors

Wenqing Li − *Institute of Reproductive Medicine, School of Medicine, Nantong University, Nantong 226000, China;* orcid.org/0000-0002-2460-7945; Email: liwenqing505@ntu.edu.cn

Peng Zhou − *Institute of Reproductive Medicine, School of Medicine, Nantong University, Nantong 226000, China;* Email: zhoupengzp@ntu.edu.cn

Authors

Mo Wang − *Institute of Reproductive Medicine, School of Medicine, Nantong University, Nantong 226000, China*

Ya Cai − *Institute of Reproductive Medicine, School of Medicine, Nantong University, Nantong 226000, China*

Tian He − *Institute of Reproductive Medicine, School of Medicine, Nantong University, Nantong 226000, China*

Yuhang Zhang − *Institute of Reproductive Medicine, School of Medicine, Nantong University, Nantong 226000, China*

Lirong Yi − *Institute of Reproductive Medicine, School of Medicine, Nantong University, Nantong 226000, China*

Complete contact information is available at: https://pubs.acs.org/10.1021/acsomega.3c07498

Notes

The authors declare no competing financial interest.

■ ACKNOWLEDGMENTS

This work was supported by Jiangsu Specially-Appointed Professor (06200054) and the start-up fund from Nantong University.

■ REFERENCES

(1) Carlino, M. S.; Larkin, J.; Long, G. V. Immune checkpoint inhibitors in melanoma. *Lancet* **2021**, *398* (10304), 1002−1014.

(2) Dall'Olio, F. G.; Marabelle, A.; Caramella, C.; Garcia, C.; Aldea, M.; Chaput, N.; Robert, C.; Besse, B. Tumour burden and efficacy of immune-checkpoint inhibitors. *Nat. Rev. Clin. Oncol.* **2022**, *19* (2), 75−90.

(3) Propper, D. J.; Balkwill, F. R. Harnessing cytokines and chemokines for cancer therapy. *Nat. Rev. Clin. Oncol.* **2022**, *19* (4), 237−253.

(4) Briukhovetska, D.; Dorr, J.; Endres, S.; Libby, P.; Dinarello, C. A.; Kobold, S. Interleukins in cancer: from biology to therapy. *Nat. Rev. Cancer* **2021**, *21* (8), 481−499.

(5) June, C. H.; O'Connor, R. S.; Kawalekar, O. U.; Ghassemi, S.; Milone, M. C. CAR T cell immunotherapy for human cancer. *Science* **2018**, *359* (6382), 1361−1365.

(6) Irvine, D. J.; Maus, M. V.; Mooney, D. J.; Wong, W. W. The future of engineered immune cell therapies. *Science* **2022**, *378* (6622), 853−858.

(7) Li, W.; Zhang, X.; Zhang, C.; Yan, J.; Hou, X.; Du, S.; Zeng, C.; Zhao, W.; Deng, B.; McComb, D. W.; Zhang, Y.; Kang, D. D.; Li, J.; Carson, W. E., 3rd; Dong, Y. Biomimetic nanoparticles deliver mRNAs encoding costimulatory receptors and enhance T cell mediated cancer immunotherapy. *Nat. Commun.* **2021**, *12* (1), No. 7264.

(8) Kaufman, H. L.; Kohlhapp, F. J.; Zloza, A. Oncolytic viruses: a new class of immunotherapy drugs. *Nat. Rev. Drug Discovery* **2015**, *14* (9), 642−662.

(9) Bommareddy, P. K.; Shettigar, M.; Kaufman, H. L. Integrating oncolytic viruses in combination cancer immunotherapy. *Nat. Rev. Immunol.* **2018**, *18* (8), 498−513.

(10) Labrijn, A. F.; Janmaat, M. L.; Reichert, J. M.; Parren, P. Bispecific antibodies: a mechanistic review of the pipeline. *Nat. Rev. Drug Discovery* **2019**, *18* (8), 585−608.

(11) Liu, Y.; Wang, L.; Song, Q.; Ali, M.; Crowe, W. N.; Kucera, G. L.; Hawkins, G. A.; Soker, S.; Thomas, K. W.; Miller, L. D.; Lu, Y.; Bellinger, C. R.; Zhang, W.; Habib, A. A.; Petty, W. J.; Zhao, D. Intrapleural nano-immunotherapy promotes innate and adaptive immune responses to enhance anti-PD-L1 therapy for malignant pleural effusion. *Nat. Nanotechnol.* **2022**, *17* (2), 206−216.

(12) Nam, J.; Son, S.; Park, K. S.; Zou, W. P.; Shea, L. D.; Moon, J. J. Cancer nanomedicine for combination cancer immunotherapy. *Nat. Rev. Mater.* **2019**, *4* (6), 398−414.

(13) Yum, S.; Li, M.; Chen, Z. J. Old dogs, new trick: classic cancer therapies activate cGAS. *Cell Res.* **2020**, *30* (8), 639−648.

(14) Wu, J. X.; Sun, L. J.; Chen, X.; Du, F. H.; Shi, H. P.; Chen, C.; Chen, Z. J. J. Cyclic GMP-AMP Is an Endogenous Second Messenger in Innate Immune Signaling by Cytosolic DNA. *Science* **2013**, *339* (6121), 826−830.
(15) Ishikawa, H.; Ma, Z.; Barber, G. N. STING regulates intracellular DNA-mediated, type I interferon-dependent innate immunity. *Nature* **2009**, *461* (7265), 788−792.
(16) Fitzgerald, K. A.; McWhirter, S. M.; Faia, K. L.; Rowe, D. C.; Latz, E.; Golenbock, D. T.; Coyle, A. J.; Liao, S. M.; Maniatis, T. IKKepsilon and TBK1 are essential components of the IRF3 signaling pathway. *Nat. Immunol.* **2003**, *4* (5), 491−496.
(17) Sharma, S.; tenOever, B. R.; Grandvaux, N.; Zhou, G. P.; Lin, R. T.; Hiscott, J. Triggering the interferon antiviral response through an IKK-related pathway. *Science* **2003**, *300* (5622), 1148−1151.
(18) Zhang, X.; Shi, H. P.; Wu, J. X.; Zhang, X. W.; Sun, L. J.; Chen, C.; Chen, Z. J. J. Cyclic GMP-AMP Containing Mixed Phosphodiester Linkages Is An Endogenous High-Affinity Ligand for STING. *Mol. Cell* **2013**, *51* (2), 226−235.
(19) Sun, W. X.; Li, Y.; Chen, L.; Chen, H. H.; You, F. P.; Zhou, X.; Zhou, Y.; Zhai, Z. H.; Chen, D. Y.; Jiang, Z. F. ERIS, an endoplasmic reticulum IFN stimulator, activates innate immune signaling through dimerization. *Proc. Natl. Acad. Sci. U.S.A.* **2009**, *106* (21), 8653−8658.
(20) Zhong, B.; Yang, Y.; Li, S.; Wang, Y. Y.; Li, Y.; Diao, F. C.; Lei, C. Q.; He, X.; Zhang, L.; Tien, P.; Shu, H. B. The Adaptor Protein MITA Links Virus-Sensing Receptors to IRF3 Transcription Factor Activation. *Immunity* **2008**, *29* (4), 538−550.
(21) Woo, S. R.; Fuertes, M. B.; Corrales, L.; Spranger, S.; Furdyna, M. J.; Leung, M. Y. K.; Duggan, R.; Wang, Y.; Barber, G. N.; Fitzgerald, K. A.; Alegre, M. L.; Gajewski, T. F. STING-Dependent Cytosolic DNA Sensing Mediates Innate Immune Recognition of Immunogenic Tumors. *Immunity* **2014**, *41* (5), 830−842.
(22) Chin, E. N.; Yu, C. G.; Vartabedian, V. F.; Jia, Y.; Kumar, M.; Gamo, A. M.; Vernier, W.; Ali, S. H.; Kissai, M.; Lazar, D. C.; Nguyen, N.; Pereira, L. E.; Benish, B.; Woods, A. K.; Joseph, S. B.; Chu, A. L.; Johnson, K. A.; Sander, P. N.; Martinez-Pena, F.; Hampton, E. N.; Young, T. S.; Wolan, D. W.; Chatterjee, A. K.; Schultz, P. G.; Petrassi, H. M.; Teijaro, J. R.; Lairson, L. L. Antitumor activity of a systemic STING-activating non-nucleotide cGAMP mimetic. *Science* **2020**, *369* (6506), 993−999.
(23) Pan, B. S.; Perera, S. A.; Piesvaux, J. A.; Presland, J. P.; Schroeder, G. K.; Cumming, J. N.; Trotter, B. W.; Altman, M. D.; Buevich, A. V.; Cash, B.; Cemerski, S.; Chang, W.; Chen, Y. P.; Dandliker, P. J.; Feng, G.; Haidle, A.; Henderson, T.; Jewell, J.; Kariv, I.; Knemeyer, I.; Kopinja, J.; Lacey, B. M.; Laskey, J.; Lesburg, C. A.; Liang, R.; Long, B. J.; Lu, M.; Ma, Y. H.; Minnihan, E. C.; O'Donnell, G.; Otte, R.; Price, L.; Rakhilina, L.; Sauvagnat, B.; Sharma, S.; Tyagarajan, S.; Woo, H.; Wyss, D. F.; Xu, S.; Bennett, D. J.; Addona, G. H. An orally available non-nucleotide STING agonist with antitumor activity. *Science* **2020**, *369*, No. aba6098.
(24) Liu, J. H.; Huang, X.; Ding, J. X. Identification of MSA-2: An oral antitumor non-nucleotide STING agonist. *Signal Transduction Targeted Ther.* **2021**, *6* (1), 18.
(25) Jiang, J. L.; Zhang, M. M.; Lyu, T.; Chen, L. R.; Wu, M.; Li, R. W.; Li, H. Z.; Wang, X.; Jiang, X. Q.; Zhen, X. Sono-Driven STING Activation using Semiconducting Polymeric Nanoagonists for Precision Sono-Immunotherapy of Head and Neck Squamous Cell Carcinoma. *Adv. Mater.* **2023**, *35* (30), No. 2300854.
(26) Li, Z. Y.; Wang, Z.; Bian, J. L.; Feng, X.; Pan, L. X.; Qian, Z. Y.; Liu, D. Y.; Guan, X.; Feng, L.; Song, B.; Xu, X.; Tan, N. H.; Ma, Y. Discovery of Selenium-Containing STING Agonists as Orally Available Antitumor Agents. *J. Med. Chem.* **2022**, *65*, 15048−15065.
(27) Wang, X. Y.; Guo, Z. J. Targeting and delivery of platinum-based anticancer drugs. *Chem. Soc. Rev.* **2013**, *42* (1), 202−224.
(28) Zhong, T. Y.; Yu, J.; Pan, Y.; Zhang, N.; Qi, Y. X.; Huang, Y. B. Recent Advances of Platinum-Based Anticancer Complexes in Combinational Multimodal Therapy. *Adv. Healthcare Mater.* **2023**, *12*, No. 2300253.
(29) Liu, W.; Li, X.; Wang, T.; Xiong, F.; Sun, C. R.; Yao, X. K.; Huang, W. Platinum Drug-Incorporating Polymeric Nanosystems for Precise Cancer Therapy. *Small* **2023**, *19* (21), No. 2208241.
(30) Yang, T.; Zhang, S. R.; Yuan, H.; Wang, Y.; Cai, L. X.; Chen, H. H.; Wang, X. Y.; Song, D. F.; Wang, X. H.; Guo, Z. J.; Wang, X. Y. Platinum-Based TREM2 Inhibitor Suppresses Tumors by Remodeling the Immunosuppressive Microenvironment. *Angew. Chem., Int. Ed.* **2023**, *62* (2), No. e202213337, DOI: 10.1002/anie.202213337.
(31) Cao, L.; Tian, H. X.; Fang, M.; Xu, Z.; Tang, D. S.; Chen, J.; Yin, J. Y.; Xiao, H. H.; Shang, K.; Han, H. B.; Li, X. P. Activating cGAS-STING pathway with ROS-responsive nanoparticles delivering a hybrid prodrug for enhanced chemo-immunotherapy. *Biomaterials* **2022**, *290*, No. 121856.
(32) Paffenholz, S. V.; Salvagno, C.; Ho, Y. J.; Limjoco, M.; Baslan, T.; Tian, S.; Kulick, A.; de Stanchina, E.; Wilkinson, J. E.; Barriga, F. M.; Zamarin, D.; Cubillos-Ruiz, J. R.; Leibold, J.; Lowe, S. W. Senescence induction dictates response to chemo- and immunotherapy in preclinical models of ovarian cancer. *Proc. Natl. Acad. Sci. U.S.A.* **2022**, *119* (5), No. e2117754119.
(33) Zhang, C. Y.; Xu, C.; Gao, X. Y.; Yao, Q. Q. Platinum-based drugs for cancer therapy and anti-tumor strategies. *Theranostics* **2022**, *12* (5), 2115−2132.

https://doi.org/10.1021/acsomega.3c07498
ACS Omega 2024, 9, 2650−2656